

Classification of Ascension Island and Natal ozonesondes using self-organizing maps

Anders A. Jensen,¹ Anne M. Thompson,¹ and F. J. Schmidlin²

Received 15 July 2011; revised 26 November 2011; accepted 30 November 2011; published 17 February 2012.

[1] Ozone profiles from balloon-borne ozonesondes are used for development of satellite algorithms and in chemistry-climate model initialization, assimilation and evaluation. An important issue in the application of these profiles is how best to treat variations where varying photochemical and dynamical influences can cause the ozone mixing ratio in the tropospheric segments of the profile to change by of a factor of 2–3 within a day. Clustering techniques are an ideal way to approach the statistical classification of profile data and we apply self-organizing maps to tropical tropospheric SHADOZ data, hypothesizing that the data will sort according to various influences on ozone, namely anthropogenic sources like biomass burning, meteorological conditions, and stratospheric or extra-tropical intrusions. Self-organizing maps, that use a learning algorithm to reveal the most prominent features of a data set according to a specified number of clusters, have been determined for the 1998–2009 SHADOZ profiles over Ascension Island (512 profiles, 7.98°S, 14.42°W) and Natal, Brazil (425 profiles, 5.42°S, 35.38°W). The 2×2 self-organizing map, which creates 4 clusters, reveals that deviations from the average ozone in the free troposphere include both increased ozone resulting from seasonal biomass burning in Africa and locally reduced ozone brought about by convective lifting of unpolluted boundary-layer air. Expanding to a 4×4 self-organizing map shows how biomass burning influences the yearly cycle of tropospheric ozone at Ascension Island and captures the seasonality of ozone at both Ascension Island and Natal. Comparing Ascension Island and Natal using a 4×4 self-organizing map at each site reveals similarities in mid-tropospheric ozone, but shows differences in lower-tropospheric ozone due to Ascension Island being closer to African biomass burning and more affected by descent from the mean Walker circulation, with less convective activity, than Natal.

Citation: Jensen, A. A., A. M. Thompson, and F. J. Schmidlin (2012), Classification of Ascension Island and Natal ozonesondes using self-organizing maps, *J. Geophys. Res.*, 117, D04302, doi:10.1029/2011JD016573.

1. Introduction

1.1. Tropical Tropospheric Ozone

[2] Typical boundary-layer ozone in the tropics is about 25 parts per billion by volume (ppbv) over the Atlantic [Piotrowicz *et al.*, 1991; Thompson *et al.*, 2000; Kley *et al.*, 2007] and about 10–15 ppbv over the remote Pacific and Indian Ocean [Johnson *et al.*, 1990; Kley *et al.*, 1996; Thompson *et al.*, 1993]. Therefore, elevated concentrations of tropical boundary-layer ozone and free-tropospheric ozone are readily distinguishable against a clean background. The chemical lifetime of ozone increases with altitude due to lack of surface deposition, decrease in reaction rates, and decrease in reactants. The ozone chemical lifetime is about a month in the free troposphere [Jacob *et al.*, 1996;

Thompson *et al.*, 1996; Avery *et al.*, 2010], which spans the layer above the boundary layer and below the stratosphere. On this timescale, signatures of pollution transport or other processes are readily visible, although most studies to date have focused on 7–10-day transport [Swap *et al.*, 1996; Thompson *et al.*, 1996; Garstang *et al.*, 1996].

1.2. Biomass Burning

[3] The eastern South Atlantic is a place of particular importance in the study of ozone. Satellite imagery first called attention to a large ozone feature over the southern Atlantic [Fishman *et al.*, 1991]. The tropospheric ozone estimates from residual-based satellite techniques were verified by ozone profiles from Ascension Island (7.98°S, 14.42°W [Olson *et al.*, 1996]). Seasonal biomass burning from Africa along with prevailing low-level easterlies leads to a local total tropospheric ozone maximum from September to October in the tropical South Atlantic [Fishman *et al.*, 1991]. Both smoke and ozone plumes are concentrated at 2–10 kilometers [Diab *et al.*, 1996; Thompson *et al.*, 2011a]. Above the African pollution is a mixture of ozone that includes post-convective transport of biomass burning

¹Department of Meteorology, Pennsylvania State University, University Park, Pennsylvania, USA.

²Wallops Flight Facility, NASA Goddard Space Flight Center, Wallops Island, Virginia, USA.

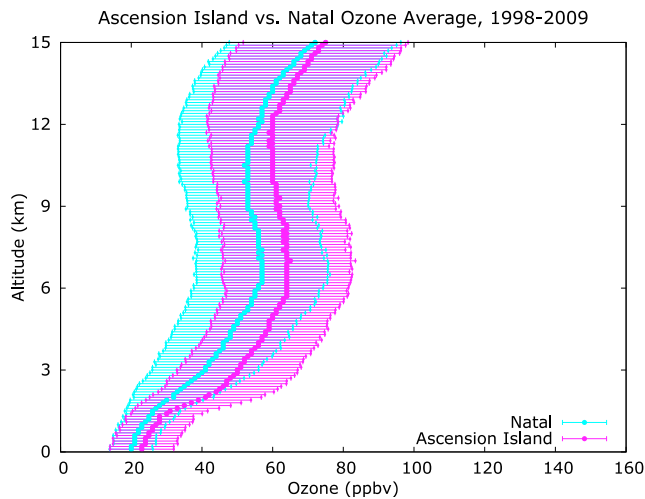


Figure 1. Mean and one standard deviation of the ozonesondes used in this analysis for Ascension Island and Natal.

emissions from Brazil [Pickering *et al.*, 1992, 1996; Thompson *et al.*, 1996, 1997]. These layers have been shown to reach the south Atlantic ozone maximum region in about 5 days, being carried in the upper troposphere [Krishnamurti *et al.*, 1993, 1996; Talbot *et al.*, 1996]. In order for this pollution to affect the middle and upper troposphere, large-scale circulation is hypothesized to produce the lifting needed to transport this pollution to the middle and upper troposphere [Watson *et al.*, 1990].

[4] In addition to biomass burning, tropospheric ozone is enhanced by lightning [Smyth *et al.*, 1996; Thompson *et al.*, 1997; Moxim and Levy, 2000] and subsidence of ozone near the tropopause in the descending branch of the Walker circulation [Krishnamurti *et al.*, 1996; Thompson *et al.*, 2000, 2011a, 2011b]. Thus, tropospheric ozone over the tropical South Atlantic is usually greater than over the north Atlantic, where circulation patterns are different [Thompson and Hudson, 1999; Martin *et al.*, 2002; Edwards *et al.*, 2003].

[5] The highest frequency of African biomass burning in the band from 10°S to 20°S occurs from July to September; these fires can be attributed to anthropogenic burning and lightning [Swap *et al.*, 1996]. Data from the 1992 Southern African Fire-Atmosphere Research Initiative (SAFARI-92) show four stable layers over Pretoria, South Africa from mid-August to early November [Garstang *et al.*, 1996]. Extreme stability of pollution during this period was established with radiosondes at several locations in southern Africa. For example, air parcels leaving Okaukuejo, Namibia (19°S, 23°E) take about a week to reach Ascension Island between 900 hPa and 800 hPa [Swap *et al.*, 1996], signifying that sustained stability is necessary for African pollution to reach Ascension Island. The first two stable layers include one associated with the top of the mixing layer at 700 hPa and a subsidence inversion at 500 hPa while the third stable layer resides at 350 hPa and the fourth is at the tropopause [Garstang *et al.*, 1996]. Normally, stability from the mixing layer is broken by westerly waves approximately every 6 days [Preston-Whyte and Tyson, 1973]. Because the transport time of pollution from Africa to the southern Atlantic Ocean is roughly the same amount of time as westerly wave passage [Diab *et al.*, 1996], a continual

source of ozone can reach the subsidence inversion from below. Once there, smoke plumes in the free troposphere tend to remain confined in stable layers and can recirculate over the African continent [Thompson *et al.*, 2002; Kahn *et al.*, 2007; Val Martin *et al.*, 2010] before horizontal transport takes the smoke toward the eastern South Atlantic [Browell *et al.*, 1996]. It is worth pointing out that although pollution enhances ozone over the tropical oceans in general [Randriambelo *et al.*, 2000; Oltmans *et al.*, 2001; Thompson *et al.*, 2007], it has been found that extra-tropical air, even stratospheric, finds its way in the troposphere [Pfister *et al.*, 2010; Selkirk *et al.*, 2010; Thompson *et al.*, 2010].

1.3. Goals and Approach of Study

[6] In summary, there are many factors contributing to tropospheric ozone over the tropics, including horizontal transport, stratospheric influence, in-situ photochemical production from precursors originating from biomass burning and other anthropogenic processes, and even biogenic sources. With the multiple effects on vertical ozone distribution and the amount of available data, for example, over 5000 tropical and sub-tropical profiles in the Southern Hemisphere Additional Ozonesondes (SHADOZ) data set [Thompson *et al.*, 2003a, 2011b], there are a number of ways to develop climatologies of tropospheric ozone profiles. Annual and seasonal means have been used from SHADOZ profiles, sometimes zonally averaged [McPeters *et al.*, 2007], in other cases, retained for individual locations (A. M. Thompson *et al.*, SHADOZ (Southern Hemisphere Additional Ozonesondes) ozone climatology (2005–2009): 4. Tropospheric and lower stratospheric profiles with comparisons to OMI total ozone, submitted to *Journal of Geophysical Research*, 2012). Signatures of oscillations on the timescale of the El Niño-Southern Oscillation (ENSO) [Randel and Thompson, 2011], the Indian Ocean Dipole [Thompson *et al.*, 2001] and the Quasi-biennial Oscillation (QBO) [Witte *et al.*, 2008; Lee *et al.*, 2010] have also been reported using SHADOZ profiles. From the point of view of satellite algorithms and model evaluation, the Atlantic and Pacific contrasts may be significant [Thompson *et al.*, 2003b]. Thus, it is highly desirable to have a more statistically robust way to approach ozonesonde profile classification in the tropics.

[7] In this study, we apply a clustering method that uses self-organizing maps (SOMs) to test the idea that the different clusters can be explained by certain meteorological phenomena. We create SOMs for ozonesondes launched at both Ascension Island and Natal, Brazil (5.42°S, 35.38°W), two south Atlantic stations with more than 400 profiles each. Although the two sites are only 2300 kilometers apart and are climatologically similar in terms of ozone mixing ratio (Figure 1), seasonal changes in various aspects of meteorology and biomass burning from Africa are expected to lead to subtle differences as well as similarities on ozone concentrations. While clustering ozonesondes is not new [see Diab *et al.*, 2003, 2004], the SOMs technique [Phahlane, 2007] provides significant advantages compared to other methods. Clustering with SOMs allows for missing data; ozonesonde profiles can include data gaps and still be used in creating SOMs. SOMs start with a predetermined map size, where the map size is the number of ozonesonde profile clusters to create, and each cluster is called a SOM node.

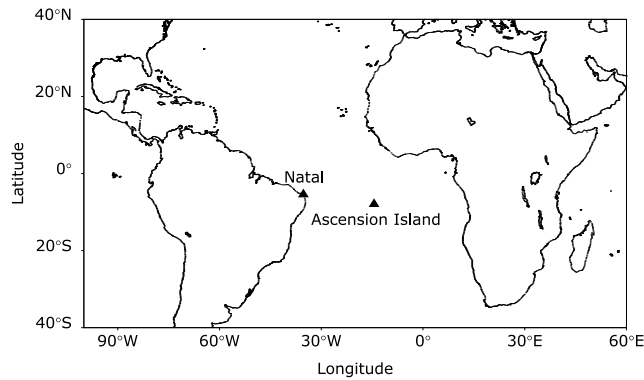


Figure 2. Ascension Island and Natal.

The map then objectively learns from the input data. Therefore, instead of starting with all the ozonesonde profiles in a group and dividing out clusters, or starting with each ozonesonde profile as its own cluster and combining similar clusters, certain SOM nodes gain information from the input data. We only specify a cluster number and make no prior assumptions about what the final assembly of nodes will look like.

2. Methods

2.1. Ozonesondes

[8] Ozonesondes obtain standard radiosonde data along with ozone concentrations employing an electrochemical cell (ECC) that uses a buffered potassium iodide (KI) solution which reacts with ozone to determine ozone concentration. Ozonesonde profiles analyzed here were taken by Science Pump 6A type ozonesondes with a 1% buffered KI solution launched at Ascension Island [Thompson *et al.*, 2003a]. At Natal, Science Pump 6A ozonesondes with a 0.5% buffered KI solution were launched until March of 1999; ozonesondes with a 1% KI solution have been in operation since April of 1999 [Thompson *et al.*, 2003a]. These ozonesondes are accurate to 5% and the radiosonde temperature reading, from Sippican instruments, is accurate to 0.5°C [Thompson *et al.*, 2003a]. Relative humidity errors become large at temperatures below -40°C , and relative humidity data should be ignored below -60°C , but relative humidity data is reliable to several percent up to about 12 kilometers [Thompson *et al.*, 2003a]. Comparisons in laboratory chamber experiments and in the field [Smit *et al.*, 2007; Deshler *et al.*, 2008] among various instrument types and solution strengths used at SHADOZ stations, of which Ascension Island and Natal are both, show that the Science Pump instruments with the 1% buffered KI solution, optimizes the ozone reading in the troposphere [Thompson *et al.*, 2007, 2011b].

2.2. Data

[9] The data for this analysis spans ozonesondes launched at Ascension Island and Natal from 1998 to 2009 (Figure 2). The data are available in the Southern Hemisphere Additional Ozonesondes (SHADOZ) data set (<http://croc.gsfc.nasa.gov/shadoz/>).

[10] To create the self-organizing maps, ozone data was first averaged into 100-meter bins. Bins with no data for a

given launch were filled with linearly interpolated data provided the missing data spanned 500 meters or less. Data gaps that were too large over which to interpolate were included as missing data because the SOM algorithm handles missing data by leaving it out of all calculations, and therefore missing data does not affect the SOM as a whole [Kohonen, 1995].

3. Self-Organizing Maps

[11] Mathematically, a SOM is a mapping from an input data space onto a two-dimensional array of nodes where each node of a self-organizing map contains information about the input data; for mathematical details, refer to Kohonen [1995]. Each node is representative of the input data and therefore each node can be visualized exactly like the input data. The end result of the SOM learning process is to have an array of nodes that represent the input data, where the array of nodes is arranged such that different data clusters become visible. In order to learn from the input data, every SOM node has a parametric reference vector with which it is associated, and these reference vectors must be initialized either randomly or in some ordered state. For example, the reference vectors can be linearly initialized in the direction of the two largest variances in the data [see Kohonen, 1995]. Reference vectors are the initial values of each SOM node, and reference vectors are required so that the SOM nodes can be visualized like the input data.

[12] After initialization, some stochastic input vector is compared to every reference vector and the closest match, named the best-matching unit (BMU), is determined by a given distance metric, usually Euclidean. The Euclidean distance between an ozonesonde profile having ozone values x_1, x_2, \dots, x_n at height levels 1, 2, \dots, n and a reference vector r_1, r_2, \dots, r_n is $\sqrt{(x_1 - r_1)^2 + (x_2 - r_2)^2 + \dots + (x_n - r_n)^2}$. Therefore, after the Euclidean distance between an input vector and each reference vector is computed, the BMU can be determined by the smallest Euclidean distance.

[13] Each reference vector is then updated so that the BMU and reference vectors within a certain distance of the BMU become more like the input vector. This is how the SOM becomes representative of the input data. Whether or not a reference vector learns from the input vector is determined by the neighborhood function, where the neighborhood function is defined in terms of distance from the BMU, its width, and a learning rate factor [Kohonen, 1995]. The learning rate factor can be between 0 and 1 and is a multiplicative factor that determines how much reference vectors learn. The learning rate factor decreases in time to help ensure node arrangement is not lost once it is attained [Kohonen, 1995]. An example of a neighborhood function is a Gaussian function where reference vectors that are far away from the BMU do not learn from that particular input vector. This is how the data clusters come about in SOMs. Because of the neighborhood function, only reference vectors that are topologically close enough to the BMU will be updated according to the SOM learning algorithm. Certain nodes learn more from certain input vectors than others and nodes that learn from similar input vectors become grouped adjacently. For computational efficiency, the entire data set can be presented to the SOM during each learning iteration

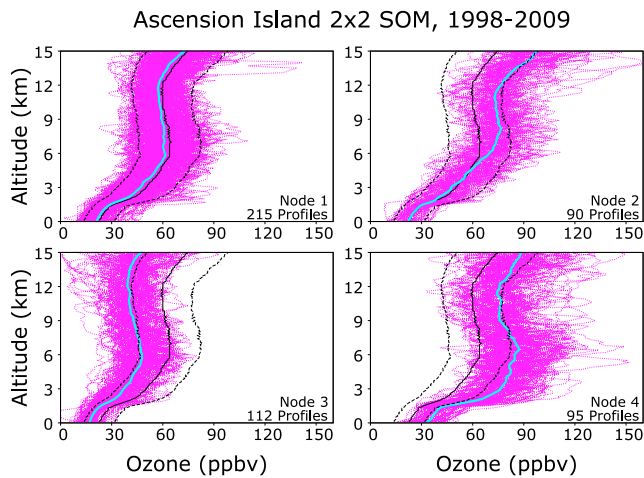


Figure 3. A 2×2 SOM (cyan) and all the ozonesonde profiles (magenta) from Ascension Island between 1998 and 2009 that had each node as a BMU. The average ozone and one standard deviation for the entire period are plotted in solid black and dashed black respectively.

instead of single data vectors which is known as batch training. That method was implemented for this analysis.

[14] The SOM learning process is iterative and the final SOM quality is measured by two errors. The mean quantization error is the average distance between each input vector and its BMU [Kohonen, 1995]. The topographic error is the proportion of all data vectors for which the first and second BMUs are not adjacent [Kiviluoto, 1996]. The mean quantization error measures how well the SOM fits the input data; a smaller mean quantization error means each data vector is close to a SOM node and therefore the SOM nodes represent the data well. The topographic error measures how well the map is ordered. Using different parameters including the neighborhood function and learning rate factor can act to increase or decrease these errors, but if the SOM network is not large then the selection of process parameters is not very crucial [Kohonen, 1995].

[15] We start by creating a 2×2 SOM for both locations and then expand the number of SOM nodes to determine how changing the number of SOM nodes affects the output display. A SOM with more nodes should include clusters with smaller differences in ozone as compared to a SOM with fewer nodes, but a SOM with fewer nodes should display ozone differences on larger timescales, like seasonal differences. Therefore, a 2×2 SOM will be shown to provide enough information for our analysis using the smallest amount of nodes, and a 4×4 SOM provides a better look at smaller scale differences. A 4×4 SOM includes 16 nodes. Because the data analyzed from Natal includes 425 profiles, increasing the number of SOM nodes beyond 16 will stretch the data too thin and defeat the purpose of being able to easily visualize the clusters. Therefore, the largest SOM created for this analysis is a 4×4 SOM.

[16] While the SOM nodes themselves are useful information, SOM nodes are not real data; they learn from real data. Therefore the SOM nodes are plotted and also any ozonesonde profile that has a given node as a BMU is plotted with that node. This method of display leads to a clustering of the ozonesonde profiles. The only two pieces of information

given to the SOM are ozone values and the altitude of the ozone values; the SOM knows nothing about season or general meteorological patterns. Therefore, the SOM learns based on ozone and altitude, and other variables can be compared to the SOM to try to determine the main factors that influence the different ozone clusters. Because the SOM is sensitive to large variability, it is ideal for studying variability of free-tropospheric ozone. Therefore, SOMs were only run up to 15 kilometers in order to look at changes in free-tropospheric ozone without the influence of the large ozone increase in the tropical tropopause layer (TTL).

4. Results of Self-Organizing Maps for Ascension Island

[17] The Ascension Island self-organizing maps were created from 512 ozonesonde profiles that were all launched between 12 and 16 UTC. Imposing this time limit minimizes photochemical ozone effects in the boundary layer and allows the SOMs to pick out differences in ozone caused by other processes.

4.1. The 2×2 Ascension Island Self-Organizing Map

[18] A 2×2 SOM using the Ascension Island data is shown in Figure 3. The SOM nodes are plotted in cyan and the ozonesonde profiles that had a specific SOM node as a best-matching unit (BMU) are plotted in magenta. The average ozone and one standard deviation for the entire period are plotted in solid black and dashed black respectively. The SOM reveals four distinct profile types. Node 1 is a BMU for 215 profiles or 42% of the profiles. Node 1 is very similar to the mean ozone during the entire period and the profiles used to create this node span the entire year when ozonesonde launch month versus year is plotted for each SOM node (Figure 4, top left). Node 1 is interpreted as representing the typical equilibrium amount of ozone that exists owing to the chemical lifetime of ozone. This grouping exhibits low boundary-layer ozone with increased ozone in the free troposphere where the chemical lifetime of ozone is longer.

[19] Node 3 imitates the characteristic tropical “S”-shape [Folkins *et al.*, 2002] with depleted ozone in the boundary layer, increasing ozone concentration in the middle troposphere, a local minimum at the level of convective outflow, and increasing ozone above the convective outflow that extends into the stratosphere [Avery *et al.*, 2010; Thompson *et al.*, 2011b]. This node is a BMU for 112 profiles, which makes up 22% of the Ascension Island profiles. Node 3 learned from ozonesondes that mainly occur in Autumn in the Southern Hemisphere, when average surface-based convective available potential energy (CAPE) is near its yearly maximum. Convective outflow in the tropics usually occurs between 10 and 14 kilometers, and the local minimum that shows up in SOM node 3 near 12 kilometers confirms that convective outflow of low-ozone air can be a dominant feature in ozonesonde profiles. Because the chemical lifetime of ozone is greater than convective timescales, locally low ozone concentrations should be seen at convective outflow levels [Kley *et al.*, 2007]. Ozone values at convective outflow levels are not as small as surface ozone values which suggests that convective outflow parcels sometimes come from 2–3 kilometers [Avery *et al.*, 2010].

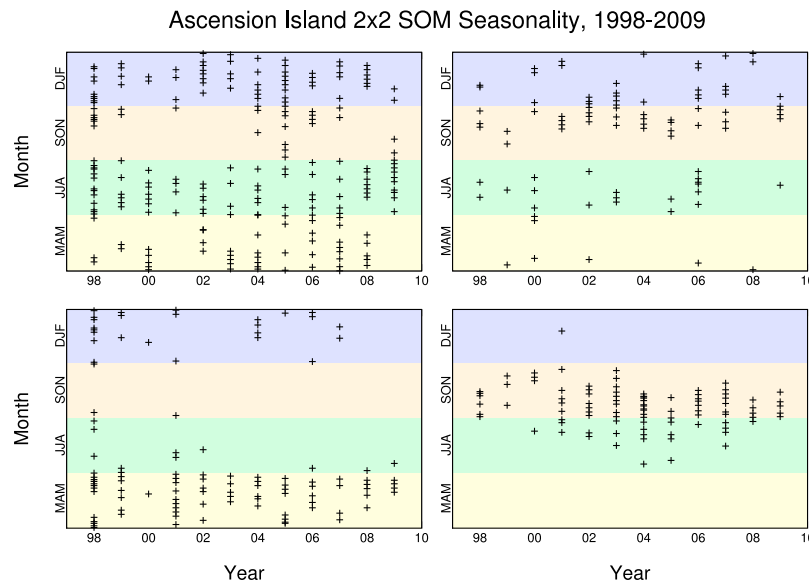


Figure 4. The month and year of all of the ozonesonde profiles that went into each node of the SOM. The months are divided into meteorological seasons: March, April, May (MAM), June, July, and August (JJA), September, October, November (SON), and December, January, February (DJF). The positions of the plots correspond to the positions of the SOM nodes in Figure 3.

Therefore, node 3 includes ozonesonde profiles that are similar to what is theorized during the convective season, with lower ozone at convective outflow levels than the average.

[20] Node 4 displays a pronounced increase of ozone above 1.5 kilometers. This increase is due to biomass burning from Africa that persists throughout Spring in the Southern Hemisphere. Increases in boundary-layer and free-tropospheric ozone make pollution in the tropics distinguishable against a clean background. The pollution seen in node 4 is responsible for the increased surface ozone as well as the increased ozone that becomes trapped above an inversion around 1.5 kilometers at an altitude where the chemical lifetime of ozone is higher than at the surface. Node 4 includes 95 profiles, which makes up about 19% of the total profiles, that persist mainly from June to November (Figure 4, bottom right).

[21] Node 2 includes the profiles that were not BMUs for any of the other three groupings. This grouping includes profiles with similar boundary-layer ozone to the average boundary-layer ozone in the node 1. The difference is the free-tropospheric ozone in node 2 increases faster than the average. One explanation is that in the upper troposphere, ozone production is generally low, but transport of NO_x and CO into the upper troposphere can increase ozone production in this region [Pickering *et al.*, 1992; Smyth *et al.*, 1996; Thompson *et al.*, 1996]. Also, because Ascension Island is in a region of subsidence from the Walker circulation, node 2 might be a result of stratospheric influence.

[22] Average change in virtual potential temperature with respect to height ($d\theta_v/dz$) is plotted in Figure 5 for each SOM node. First, θ_v was calculated from the radiosonde data, and then θ_v was averaged into 100-meter bins before the derivative was taken. All the $d\theta_v/dz$ profiles that had a SOM node as a BMU were then averaged. Positive values indicate stable layers. The stable layer above the boundary layer exists

throughout the year leading to a persistent increase in ozone above the boundary layer. The bottom right plot corresponds to the polluted SOM node (node 4) and has the most pronounced stable layer compared to the other nodes as well as the largest ozone gradient above 1.5 kilometers. Ozone created from biomass burning in Africa travels over the southern Atlantic into a region of subsidence and builds up above this stable layer. There is a slight increase in surface ozone seen in node 4 which hints at the fact that some of the ozone from biomass burning is either being mixed down to the surface at Ascension Island or is remaining in the marine boundary layer and being carried to Ascension Island by low-level flow. However, on average, a majority of the total ozone from biomass burning resides above this stable layer.

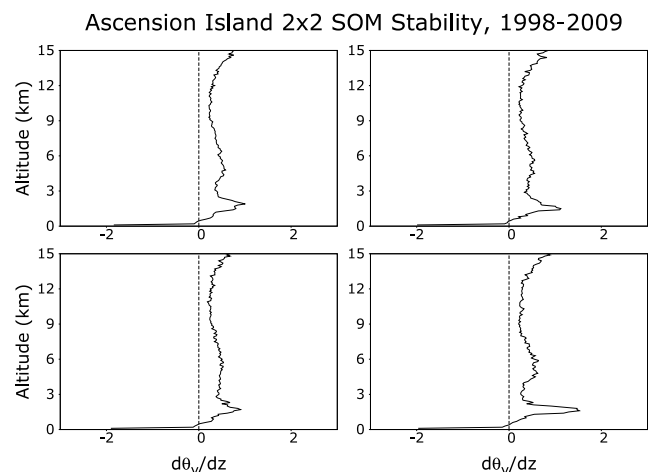


Figure 5. Average change in virtual potential temperature with height for all the profiles that went into creating each Ascension Island 2×2 SOM node (solid line). The dashed line is the zero line. Positive values indicates stable layers.

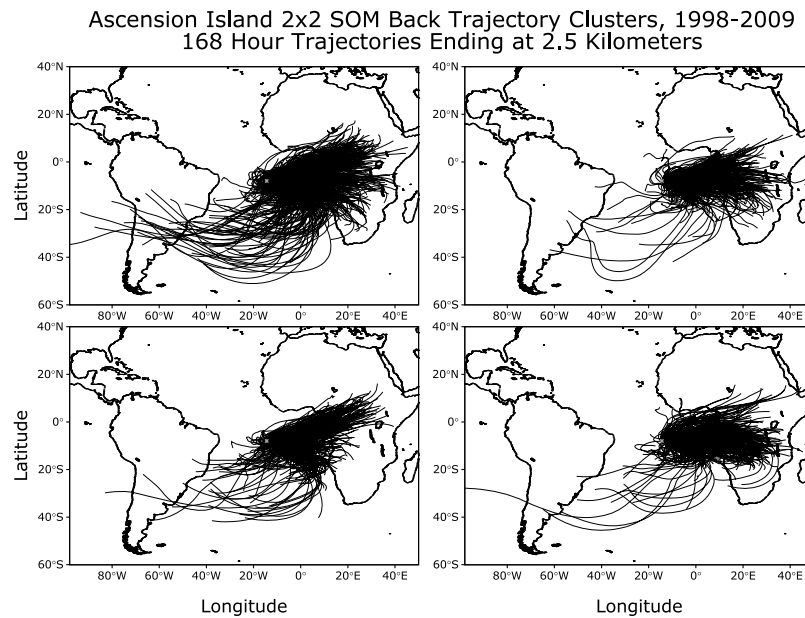


Figure 6. Seven day back trajectory clusters ending at Ascension Island at an altitude of 2.5 kilometers. Clusters correspond to the day and hour of each profile that went into making each SOM node. Ensemble back trajectories include 27 members for each day which were clustered using a 2×2 SOM. Therefore each 27-member ensemble is represented by 4 clusters. This makes the plots easier to visualize, while maintaining the statistical significance of the clusters.

[23] Seven-day back-trajectory clusters ending at 2.5 kilometers at Ascension Island are shown in Figure 6. Each seven-day back trajectory included 27 ensemble members, and these 27 ensemble members are grouped into 4 clusters. Clustering ensures that a good representation of the back trajectories remains while reducing the number of data plotted, thus making data visualization easier. The clusters are created by making a 2×2 SOM using time and altitude from the 27 back-trajectory ensemble members and then averaging the latitude and longitude of the back trajectories that were the BMU of each SOM node. Because flow patterns in the tropics are roughly dependent on altitude in the absence of convection, it is a good approximation that clustering altitude will lead to accurate position clusters.

[24] The back-trajectory clusters show that flow corresponding to the average ozone levels over Ascension Island at 2.5 kilometers (Figure 6, top left) mainly come from the African continent, with some influence from the southern Atlantic and South America. The back-trajectory clusters show that node 4 includes clusters that trace back to southern Africa during the biomass burning season with a little influence from recirculation over both southern Africa and the south Atlantic. The combination of the biomass burning, the increased stability above the boundary layer, and the subsidence from the Walker circulation leads to the increased ozone from 2.5–6 kilometers. Node 3, the least polluted of the SOM nodes at 2.5 kilometers, is influenced mainly by the south Atlantic and central Africa. The back trajectories corresponding to node 3 confirm that Ascension Island is significantly influenced by central Africa. Also, back-trajectory clusters corresponding to node 3 that remain zonal either do not cross the African continent or recirculate in the anticyclone. Because most of the profiles that had

node 3 as a BMU occur when monthly average CAPE is highest, the decrease in 2.5-kilometer ozone could also be partly from vertically mixing ozone which decreases vertical ozone gradients. Also, CAPE is highest when biomass burning is a minimum over southern Africa which means 2.5-kilometer ozone is already lower than it would be in SON; convection is therefore mixing low-ozone boundary-layer air with only slightly higher ozone at 2.5 kilometers leading node 3 to have the weakest vertical ozone gradient above the boundary layer. The back-trajectory clusters corresponding to node 2 should look similar to the average ozone back-trajectory clusters because node 2 is similar to the average ozone value at 2.5 kilometers.

[25] What is truly amazing about the 2×2 Ascension Island SOM is that there are not a lot of outliers and that each SOM node has a significant number of profiles from which it learns. This means that each SOM node is a statistically meaningful profile type for Ascension Island, remembering that each ozonesonde in a cluster has that SOM node as a BMU. Node 4 learned from ozone and altitude but it clustered profiles from June to November, signaling that increased ozone from African pollution is the most significant source of free-tropospheric ozone variability in this period.

4.2. The 4×4 Ascension Island Self-Organizing Map

[26] Because the SOM map is roughly a probability distribution of the data, allowing 4 nodes to span the entire data is useful, but incomplete. Including more SOM nodes reveals local clusters in the data. This is why we expand the number of SOM nodes in the following analysis. The 2×2 SOM maps gives us 4 distinct clusters of the data, but changes within this general representation will only arise by expanding the SOM map. Analysis of a 3×3 SOM is

Ascension Island 4x4 SOM, 1998-2009

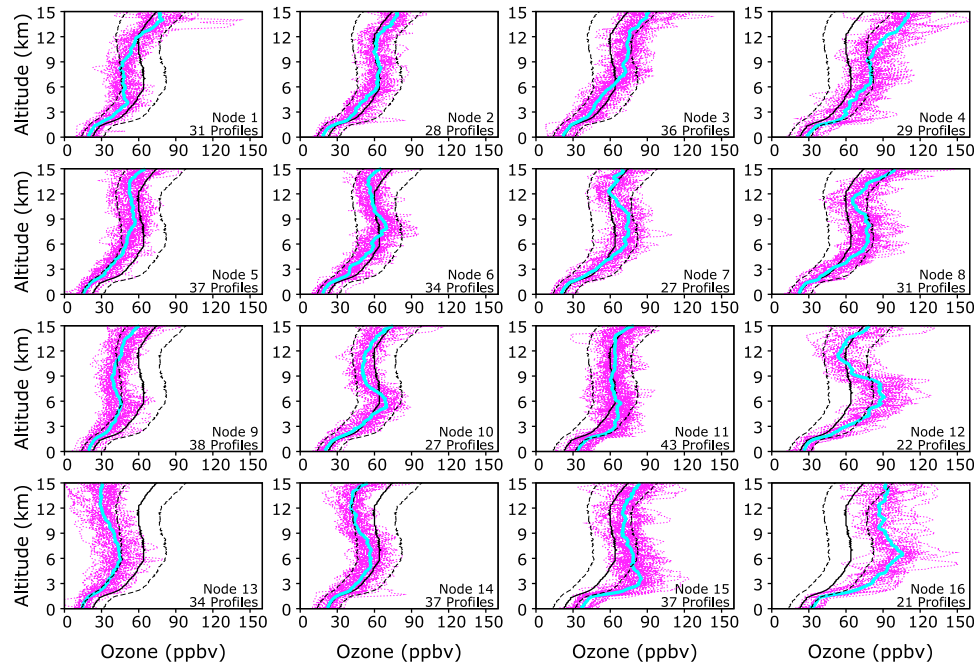


Figure 7. A 4×4 self-organizing map (cyan) and all the ozonesonde profiles (magenta) from Ascension Island between 1998 and 2009 that were used to create the SOM. The average ozone and one standard deviation for the entire period are plotted in solid black and dashed black respectively.

omitted because the 3×3 SOM did not provide enough clusters to study ozone anomalies; therefore, we expand to a 4×4 SOM. Expanding the SOM nodes at Ascension Island to 4×4 reveals the faculty of the SOM to keep similar nodes close together, which is the preservation of topology. From left to right, the SOM nodes become more polluted in the lower and middle free troposphere (see Figure 7). From bottom to top, the SOM nodes become more polluted above about 9 kilometers. Also the biomass burning node (node 4) and the equilibrium ozone node (node 1) from the 2×2 SOM are now divided among many nodes.

[27] The results of a 4×4 SOM for Ascension Island further break down the profiles into more unique nodes, but each node still learns from a significant number of profiles (Figure 7). The seasonality of the clusters still reveals biomass burning profiles (Figure 8) and convectively influenced profiles. At this point, the evolution of ozone over three seasons is evident (Figure 9).

[28] Node 9 includes profiles mainly from MAM when average CAPE is high and when vertical transport of ozone allows ozone to be more evenly vertically mixed. Node 11 includes profiles mainly from JJA when biomass burning starts to increase 1.5–6-kilometer ozone. Node 15 includes a transition from JJA to SON when 1.5–3-kilometer ozone greatly increases, and ozone is elevated in general to 15 kilometers. Node 16 includes profiles mainly from SON, the middle to end of the biomass burning season, when ozone is greatly elevated across the whole profile with a local maximum in ozone just above 6 kilometers.

[29] Node 14 learned from very few ozonesonde profiles from SON (Figure 8) and has decreased stability above the boundary layer as compared to node 16, for example. Node 14 displays low upper tropospheric ozone (Figure 7)

with a local minimum in ozone between 12 and 14 kilometers which are signs of convective mixing. The 4×4 stability plot (not shown) further confirms the role stability plays at keeping ozone levels elevated above 2.5 kilometers. The nodes with the largest gradients of ozone above about 1.5 kilometers show the most pronounced stable layer at that level. Node 9 includes profiles from MAM that lack the convective signature of the local minimum in ozone at approximately 12 kilometers. These profiles occur when biomass burning is at a minimum and this should be a good approximation of what a tropical background ozone profile should look like in the absence of convection and pollution. Node 8 includes profiles near the end of the biomass burning season, and whereas lower free tropospheric ozone has returned to average values, 4–12-kilometer ozone remains above average.

[30] The 4×4 SOM seasonality suggests that ozone concentrations are first elevated above the boundary-layer and as the burning season continues, elevated ozone appears in the middle troposphere. Because the chemical lifetime of ozone increases with height in the free troposphere, this makes sense considering the continual source of ozone from burning. This is reinforced by effective lifting mechanisms including convection coupled with subsidence that can help maintain large concentrations of ozone in the middle to upper troposphere. Because of the strength of the boundary layer inversion, convection that penetrates this level should be strong enough to break any subsidence inversion and reach convective outflow levels. Therefore, convective mixing on average should bring low-ozone boundary-layer air to above 8 kilometers, allowing for mid-level ozone to remain higher than both boundary-layer and upper-tropospheric values.

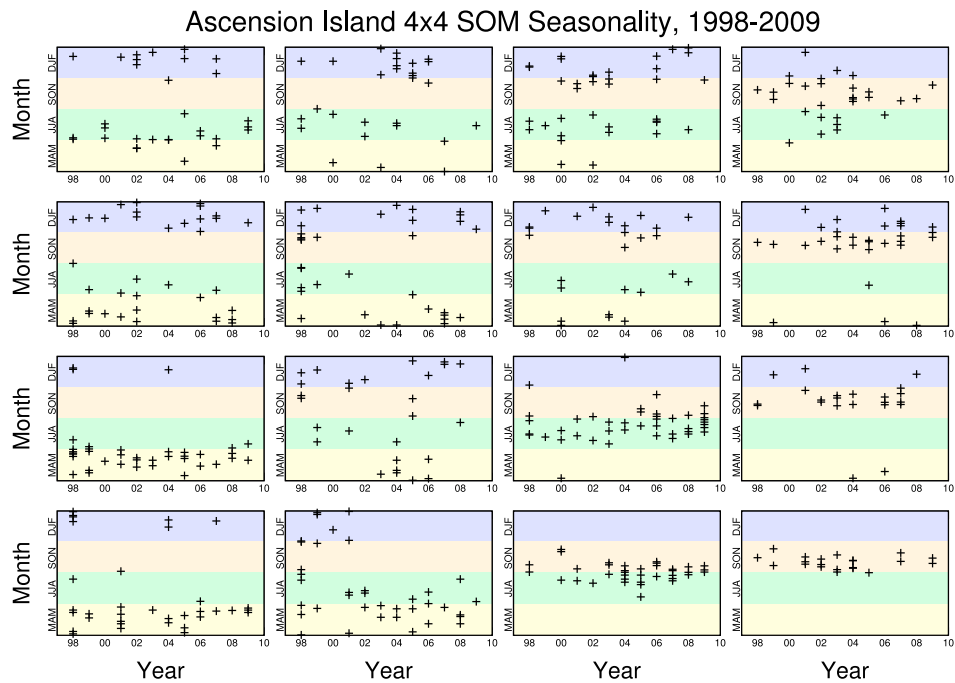


Figure 8. The month and year of all of the ozonesonde profiles that went into each node of the SOM in Figure 7. The months are divided into meteorological seasons: March, April, May (MAM), June, July, and August (JJA), September, October, November (SON), and December, January, February (DJF).

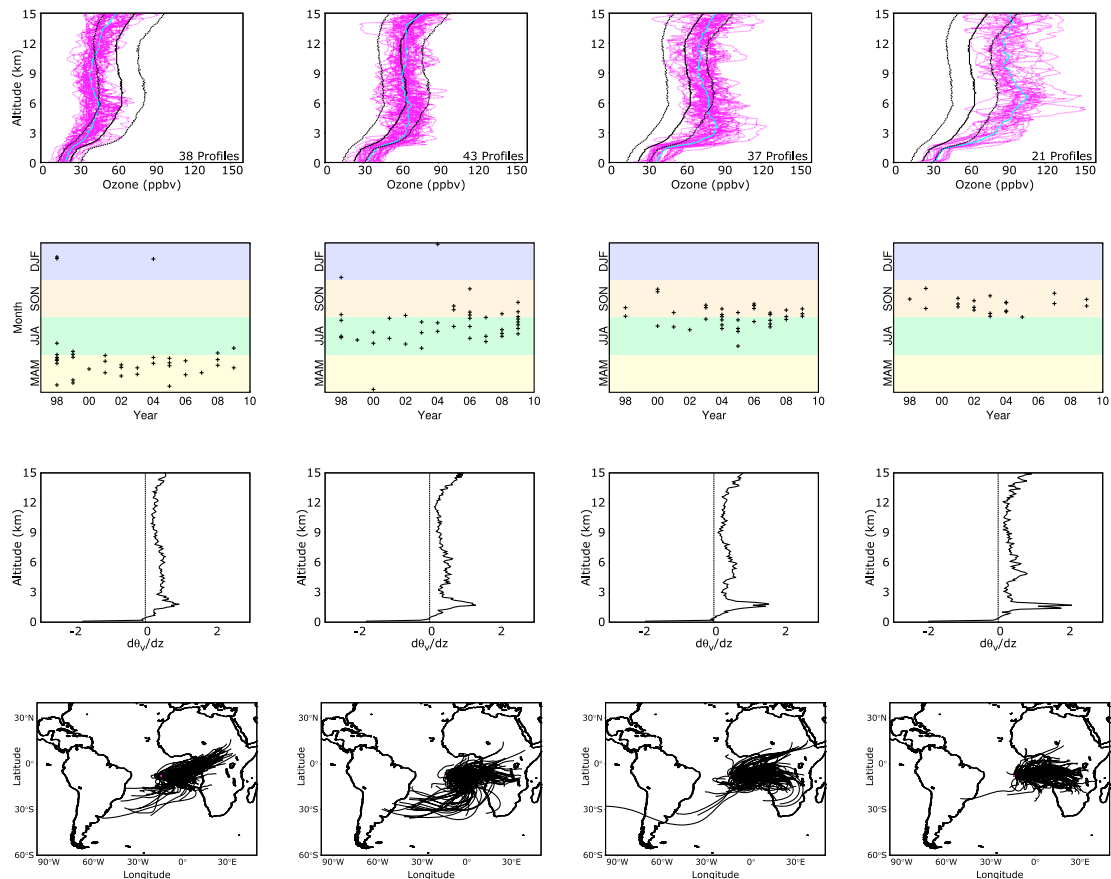


Figure 9. The yearly evolution of ozone at Ascension Island, based on the 4×4 SOM. (left to right) Nodes 9, 11, 15, 16 are plotted with corresponding seasonality, stability, and back trajectories ending at 2.5 kilometers plotted below.

Table 1. Deviation From the Mean Ozone (in ppbv) for Each SOM Node at Different Heights^a

Node	1.0 km	2.5 km	6.5 km	12.0 km
1	-4.1	-7.8	-17.2	-0.2
2	-5.1	-6.1	-2.3	2.8
3	-1.0	-5.0	0.3	15.6
4	7.0	11.2	16.0	32.4
5	-7.9	-14.2	-13.5	-7.4
6	-5.1	-7.5	-4.4	-3.1
7	-2.4	-4.7	8.0	-0.1
8	-1.4	-3.6	12.9	10.5
9	-4.6	-11.8	-20.0	-14.1
10	-2.6	-3.6	3.1	-5.7
11	11.1	13.5	0.3	3.7
12	2.3	7.0	26.8	-4.0
13	-10.0	-15.5	-19.6	-30.2
14	-1.4	-5.1	-7.9	-19.0
15	14.7	29.9	14.5	11.2
16	10.0	25.5	41.8	26.9

^aBoldface signifies where deviations exceed one standard deviation of the mean.

[31] Using 16 SOM nodes effectively shows the seasonal evolution of ozone over Ascension Island during a yearly cycle and breaks down the season in a way that shows how sensitive ozone concentrations are to tropical meteorology and advected pollution. If we compare the effects on ozone concentration between node 16 and node 9, distinct differences in season, stability, and back trajectory clusters lead to significantly different ozonesonde profiles (Figure 9, first and fourth columns). Deviations from the mean ozone for each SOM node at different heights are summarized in Table 1.

5. Results of Self-Organizing Maps for Natal

[32] The analysis of ozonesondes launched at Natal used 425 ozonesonde profiles which were launched from 1998 to 2009. Only ozonesondes that were launched between 1100 and 1600 local time were used. This minimizes changes in boundary-layer ozone that arise from launching at different times.

5.1. The 2×2 Self-Organizing Map for Natal

[33] The result of a 2×2 SOM for the data from 1998 to 2009 are shown in Figure 10. Node 3 for Natal corresponds to an average-type ozone where 35% or 150 of the profiles had that SOM node as a best-matching unit. Similar to the 2×2 Ascension Island SOM node 1, the Natal SOM node 3 closely resembles the mean of all Natal ozone profiles. Node 2 for Natal is similar to node 2 for Ascension Island except that at Ascension Island the SOM node follows the mean until 5 kilometers and then increases faster than the mean ozone, where at Natal the SOM node deviates from the mean at about 3 kilometers.

[34] Node 1 for Natal reveals the “S”-shaped convective profile where the SOM node shows considerably lower ozone than the mean throughout the profile. These profiles occurred mainly in MAM (Figure 11) which is expected because this is the convective season.

[35] Node 4 reveals profiles with ozone that is higher than the mean throughout the entire profile although this SOM node does return to within one standard deviation of the

mean at approximately 11 kilometers. This node is similar to the polluted node for Ascension Island except, as expected, the ozone gradient above the boundary layer is not as large. This lesser ozone gradient is due to Natal being farther away from African biomass burning and being more convective than Ascension Island.

[36] Node 2 includes no profiles from MAM and node 4 only includes one profile from MAM, which occurs in early March. Both nodes 2 and 4 were BMUs for 77 profiles or 18% of the data. The seasonality at Natal is similar to Ascension Island, with elevated ozone centered around SON and low ozone for profiles launched in MAM. This consistent seasonality could be used to select profiles for chemical transport models or first guess for satellite algorithms where initial conditions of ozone in Natal during MAM can be set to node 3 for average ozone or node 1 if convective.

[37] Both the 2×2 SOMs for Ascension Island and Natal have an average ozone node, one node with one standard deviation less ozone than the mean for the whole profile, and one node with one standard deviation more ozone than the mean for the whole profile. This similarity is a consequence of the SOM being like a probability distribution and also the rigidity of the SOM map. Because the nodes are connected where not just one node learns at a time, using fewer nodes means the map is more centered around the majority of the data. This explains why both 2×2 SOMs for Ascension Island and Natal look similar with respect to their means and standard deviations. The fact that the seasonality is strong for both locations validates the use of the 2×2 SOM.

5.2. The 4×4 Self-Organizing Map for Natal

[38] The 4×4 SOM for Natal shows some seasonal dependence, where nodes 1 and 2 occur mainly in MAM and DJF and nodes 12, 14, 15, and 16 are centered around the SON season (Figures 12 and 13). Nodes 1 and 2 show lower levels of ozone throughout the whole profile and nodes 12, 14, 15, and 16 all show elevated pollution at some point in the profiles. Whereas Natal does not have as significant an ozone increase above the boundary layer as Ascension

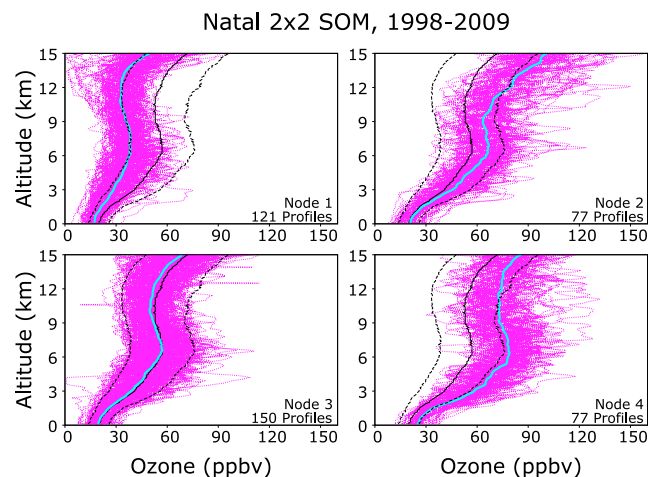


Figure 10. A 2×2 SOM (cyan) and all the Natal ozonesonde profiles (magenta) from between 1998 and 2009 that were used to create each node of the SOM. The average ozone and one standard deviation for the entire period are plotted in solid black and dashed black respectively.

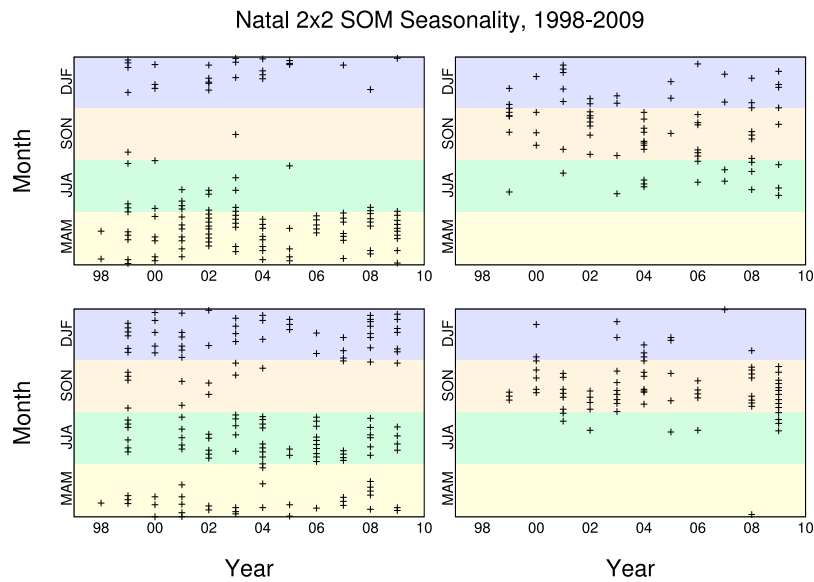


Figure 11. The month and year of all of the Natal ozonesonde profiles that went into each node of the SOM. The months are divided into meteorological seasons: March, April, May (MAM), June, July, and August (JJA), September, October, November (SON), and December, January, February (DJF). The positions of the plots correspond to the positions of the SOM nodes.

Island, Natal does show similar local maxima in ozone just above 6 kilometers, as seen in nodes 13 and 14 (Figure 12).

[39] Whereas node 2 was the BMU for 43 profiles, more profiles than any other node, node 15 was the BMU for 40 profiles and shows ozone concentrations one standard deviation above the average for the whole profile. Node 2 appears to be what a Natal sounding would look like without the influence of convection or pollution. As with Ascension Island, this node is denoted the clean background. Node 15 shows that increased ozone throughout the entire troposphere is a fairly significant occurrence at Natal because

node 15 was the BMU for 40 profiles, or 9% of the profiles. Similar to Ascension Island, nodes 15 and 16 for the 4×4 SOM are the nodes with the highest ozone concentrations, but for Ascension Island, nodes 15 and 16 show local maxima in ozone while for Natal the increased ozone occurs over the entire profiles. Natal does have two nodes, nodes 13 and 14 that show elevated ozone at approximately 6 kilometers which is consistent with the fact that at 500 hPa Natal can be downwind of Ascension Island.

[40] As compared to Ascension Island, the 4×4 SOM for Natal shows some seasonality, but the evolution of ozone

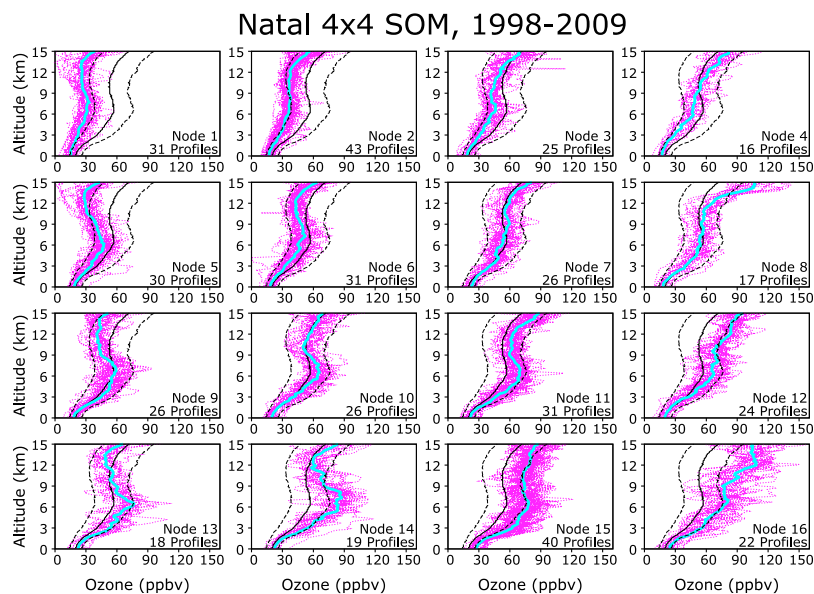


Figure 12. A 4×4 SOM (cyan) and all the Natal ozonesonde profiles (magenta) from between 1998 and 2009 that were used to create each node of the SOM. The average ozone and one standard deviation for the entire period are plotted in solid black and dashed black respectively.

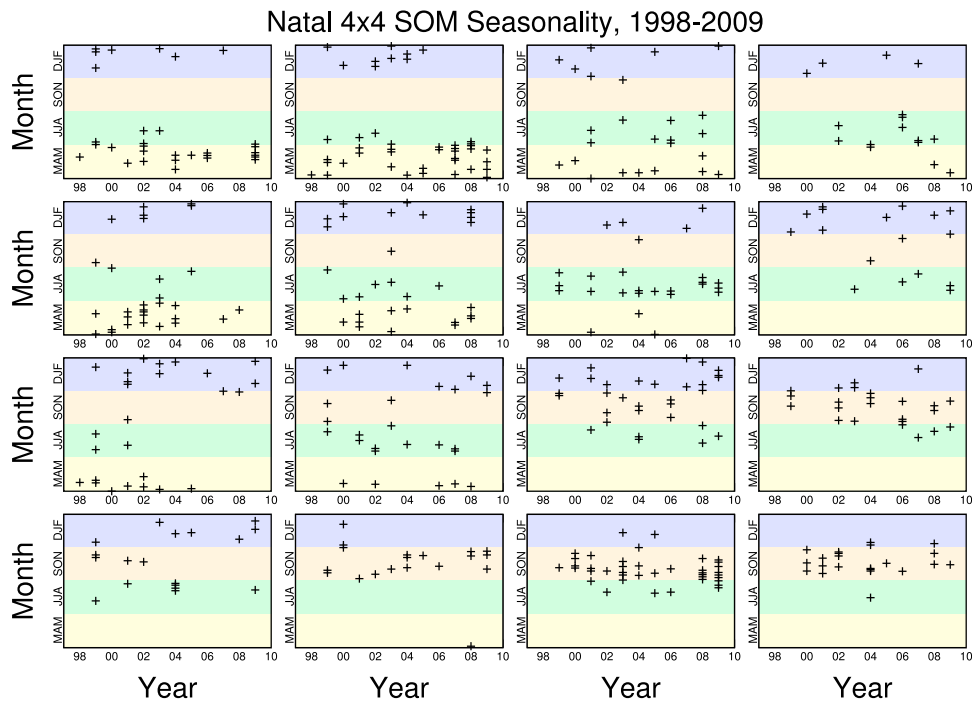


Figure 13. The month and year of all of the Natal ozonesonde profiles that went into each node of the SOM. The months are divided into meteorological seasons: March, April, May (MAM), June, July, and August (JJA), September, October, November (SON), and December, January, February (DJF). The positions of the plots correspond to the positions of the SOM nodes.

over a yearly cycle is not clear. This means that the signatures of biomass burning are not as pronounced at Natal as they are at Ascension Island. Also, the Ascension Island 4×4 SOM had only 2 nodes that included no MAM

profiles. The Natal 4×4 SOM includes 6 nodes that do not include any profiles from MAM. This is because most of the MAM profiles are clustered in the convective and less-polluted nodes toward the upper left of the SOM map. Outgoing

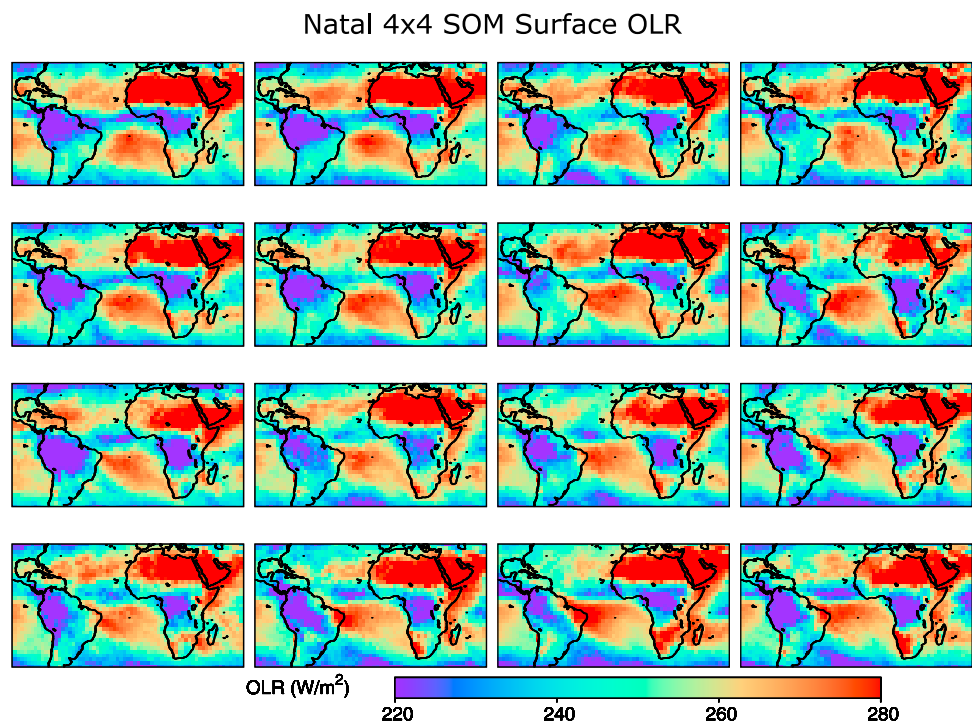


Figure 14. Surface OLR averaged for each SOM node. Data is from NCEP reanalysis.

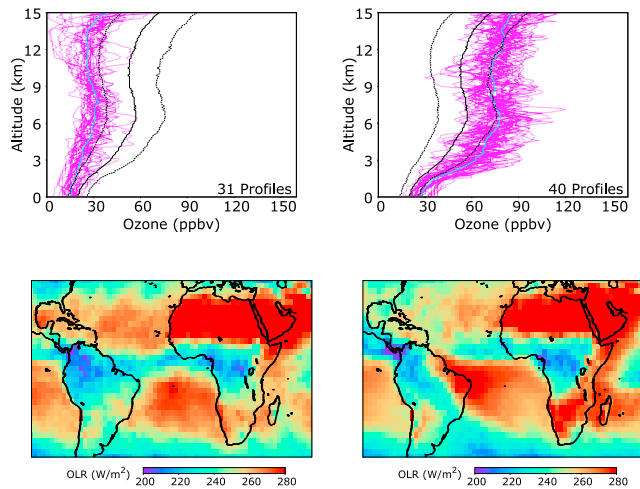


Figure 15. Node 1 and node 15 from the Natal 4×4 SOM. The corresponding OLR is plotted below. Decreased surface OLR at Natal is a sign of increased convection and this convective signature corresponds with lower ozone at convective outflow levels which is apparent in node 1. OLR values at Natal, which is denoted by the triangle, vary from approximately 240 W/m^2 corresponding to node 1 to approximately 280 W/m^2 corresponding to node 15.

longwave radiation (OLR) from National Centers for Environmental Protection (NCEP) reanalysis [Liebmann and Smith, 1996] corresponding to the 4×4 SOM at Natal verifies the convective grouping toward the upper left of the SOM where nodes 1, 2, 5, and 6 show significantly less surface OLR than nodes 11, 12, 15, and 16 (Figures 14 and 15). While the biomass burning signature in the SOM nodes is more consistently highlighted at Ascension Island, the convective signature in SOM nodes is more exclusively pronounced at Natal. The Natal 4×4 SOM leads to a pattern in MAM data that is consistent with the OLR pattern. Nodes 1, 2, 5, and 6 include almost all of the MAM launches, while nodes 11, 12, 15, and 16 include no MAM profiles (Figure 13).

[41] The 4×4 SOM for Natal also preserves topology but in a different way from the Ascension Island SOM. Here, from top to bottom, middle-tropospheric and upper-tropospheric ozone is increasing, and from left to right upper-tropospheric ozone concentrations are becoming higher than lower-

tropospheric ozone concentrations. This is different than for the Ascension Island 4×4 SOM, where the topology is less distinct, but from top to bottom local maxima become more distinguishable, and from left to right, ozone throughout the entire profiles is increasing. While SOMs try to preserve the topology, every node must go on the map so topology preservation is not always perfect. Differences in the SOM topology between Ascension Island and Natal are due to differences in ozone variability. At Ascension Island, pronounced ozone features include local maxima at 6 kilometers and the strong ozone gradient above the boundary layer, while at Natal, pronounced ozone features include low ozone due to convection and local maxima at 6 kilometers. These features are what determine the SOM topology and because some of these features are different, we expect a different SOM topology.

5.3. Results of Self-Organizing Maps for Ascension Island and Natal Combined

[42] Finally we create a 4×4 SOM using the Ascension Island and Natal data together. This SOM (not shown) confirms both the similarities and differences that exist between these two locations. The SOM nodes separate so that one node includes mostly profiles from Natal, occurring mainly in MAM, where the node is the aforementioned “S”-shaped profile. A different node includes mostly profiles from Ascension Island, occurring mainly in SON with characteristics of biomass burning influence. Most of the nodes that are not either highly influenced by convection or biomass burning show that Ascension Island and Natal are quite similar in terms of vertical ozone.

[43] At 2.5 kilometers Ascension Island and Natal for the most part are influenced by the same large scale dynamics. Increased lower-tropospheric ozone at Natal can be traced back to biomass burning in Africa as Natal back-trajectory clusters cross Ascension Island as seen in two nodes (Figure 16). Therefore, differences in ozone at 2.5 kilometers can be attributed to the increased stable layer over the boundary layer over Ascension Island, proximity to biomass burning, mean flow, and differences in frequency of convection. Similar dynamics leads to similar back trajectory clusters at 6.5 kilometers as well. Some of the Natal back trajectory clusters cross South America and circulate over Ascension Island and then end at Natal which is why the profiles at Ascension Island and Natal are clustered in the same SOM node (Figure 17).

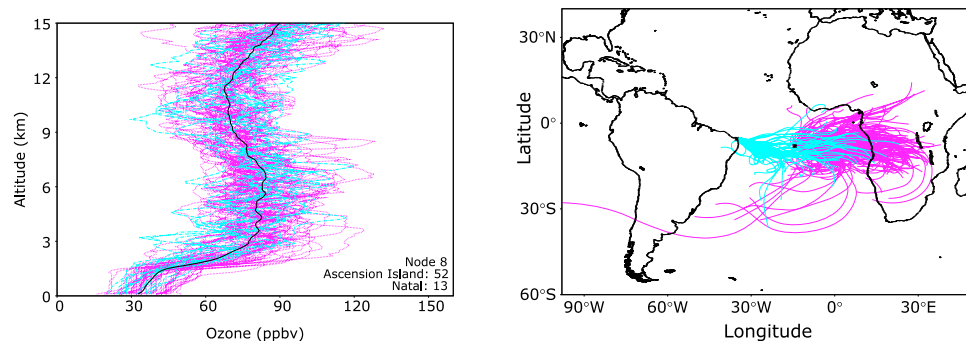


Figure 16. (left) Node 8 from the 4×4 SOM using both Ascension Island (magenta) and Natal (cyan) ozonesondes. (right) The corresponding back trajectory cluster ending at 2.5 kilometers.

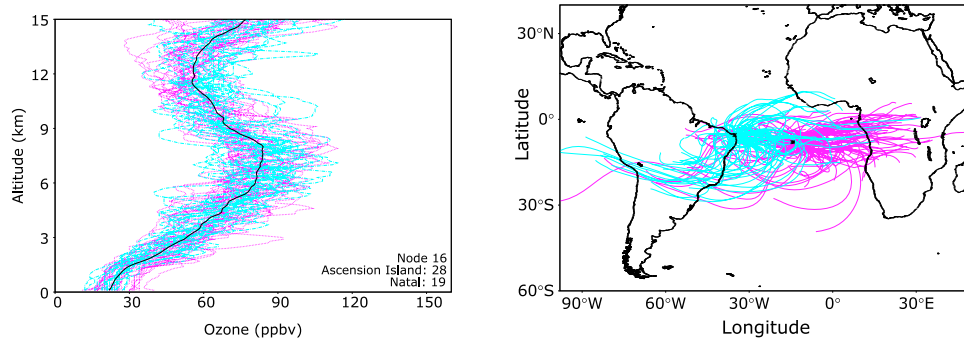


Figure 17. (left) Node 16 from the 4×4 SOM using both Ascension Island (magenta) and Natal (cyan) ozonesondes. (right) The corresponding back trajectory cluster ending at 6.5 kilometers.

[44] The Natal ozonesonde profiles that have node 8 (Figure 16, left) as a BMU occur mainly in SON and show the link between Ascension Island and Natal. These Natal ozonesonde profiles have similar back trajectory clusters at 2.5 and 6.5 kilometers as the Ascension Island profiles that had node 8 as a BMU. Therefore, the increased ozone at both locations appear to be from the same source.

[45] Eleven out of sixteen SOM nodes show similarities between the locations, while five nodes show the differences. Most of the nodes that learned from near equal percentages of ozonesonde profiles from both locations show similar back trajectory clusters ending at 6.5 kilometers. While zonal flow in the middle troposphere is common, two of the SOM nodes with the highest 6.5-kilometer ozone, which are nodes 3 and 16, show recirculation over the southern Atlantic where ozone can build up and affect both Natal and Ascension Island. Therefore, 6.5-kilometer ozone at Ascension Island and Natal is well linked and deviations of ozone at 6.5 kilometers between the locations should not persist for longer than a few weeks.

6. Conclusions

[46] We have demonstrated that self-organizing maps are a valuable statistical tool to determine meteorological and chemical variability in free-tropospheric ozone over Ascension Island and Natal. Seasonal effects on ozone over Ascension Island and Natal are apparent using four SOM nodes. A progression of seasonal effects responding to short-term meteorological influences become evident as the number of SOM nodes increases. For Ascension Island and Natal, using fewer SOM nodes results in clusters with a larger timescale; the 2×2 SOM reveals seasonal biomass burning and seasonal convection. These 2×2 SOMs demonstrate that seasonal changes in ozone are the dominant cause for variation in free-tropospheric ozone. For example, the lowest ozone, that is associated with convection, coincides with the most convectively active period at both locations, March–April–May. Over Natal, where deep convection is more active, this mechanism is consistent with small but important regional changes in cloud properties driven by the Southern Intertropical Convergence Zone [see *Grodsky and Carton, 2003*], summarized in OLR coincident with the soundings.

[47] Expanding the number of SOM nodes for Ascension Island and Natal displays clusters that are grouped by season

because SOMs preserve topology by placing similar nodes in adjacent positions. These grouping of nodes reveal inter-seasonal changes in ozone and substantial differences in free-tropospheric ozone. Details of how the biomass burning season affects ozone over Ascension Island become evident when increasing the number of SOM nodes to 16. The season starts from the build up of ozone above 1.5 kilometers and develops due to a continuous supply of ozone from biomass burning, the southern hemisphere anticyclone and convection or other lifting mechanisms. Gradually, ozone enhancements reach the middle troposphere where the chemical lifetime of ozone approaches one month. The Natal SOMs reveal that an elevated ozone layer at 6.5 kilometers that is pronounced over Ascension can end up over Natal.

[48] Comparing Ascension Island and Natal reveals meteorological features, including Ascension Island being less convective than Natal and a stronger stable layer over the boundary layer at Ascension Island. These distinctions, and a shorter transit distance from Africa to Ascension can lead to considerable differences in vertical ozone profiles. The two locations show similar profiles for a typical clean sounding and increased ozone around 6.5 kilometers. Both the similarities and differences seen in ozonesonde profiles from Ascension Island and Natal result from the timescales of the meteorological influences. The chemical lifetime of ozone increases from about a week at the surface to a month in the free troposphere while the biomass burning season is at a maximum in southern Africa for about 3 months. Also, the horizontal transport of ozone from Africa to Ascension Island takes about a week. This allows for the build up of ozone above the Ascension Island boundary layer that is seen in the yearly ozone cycle from the 4×4 SOM. Convection works to vertically mix ozone on a timescale of hours which is why ozone concentrations can remain below average and well mixed during the convective season.

[49] Self-organizing maps are a powerful tool for clustering data. Using self-organizing maps to classify ozonesondes and analyze how different meteorological phenomena influence ozone can improve evaluation and validation of coupled chemical-transport models, and climate models. Satellite algorithms, that tend to be based on simpler averages, can be improved with the use of tropospheric ozone profiles that often differ by a factor of two over seasons and regions. The tropics is an important region for ozone-temperature interactions that affect tropospheric injection of constituents in the stratosphere and stratospheric circulation. Accurate satellite

data, profile measurements, chemical and climate modeling are all important in this region. Statistical approaches based on SOMs are expected to improve both detection of ozone trends and model predictive capabilities.

[50] **Acknowledgments.** This research was supported by the Earth and Environmental Systems Institute (EESI) Environmental Scholar fund through Pennsylvania State University and the NASA SHADOZ grant NNX09AJ23G for which M. J. Kurylo and K. W. Jucks are thanked. We are grateful to the years of excellent sounding data from Russell Yon (Ascension Island), Neusa M. Paes Leme and Francisco DaSilva (INPE, Brazil). Conversations with Chris Nowotarski were exceptionally helpful.

References

- Avery, M., et al. (2010), Convective distribution of tropospheric ozone and tracers in the Central American ITCZ region: Evidence from observations during TC4, *J. Geophys. Res.*, *115*, D00J21, doi:10.1029/2009JD013450.
- Browell, E. V., et al. (1996), Ozone and aerosol distributions and air mass characteristics over the South Atlantic Basin during the burning season, *J. Geophys. Res.*, *101*(D19), 24,043–24,068.
- Deshler, T., et al. (2008), Atmospheric comparison of electrochemical cell ozonesondes from different manufacturers, and with different cathode solution strengths: The balloon experiment on standards for ozonesondes, *J. Geophys. Res.*, *113*, D04307, doi:10.1029/2007JD008975.
- Diab, R. D., et al. (1996), Vertical ozone distribution over southern Africa and adjacent oceans during SAFARI-92, *J. Geophys. Res.*, *101*(D19), 23,823–23,833.
- Diab, R. D., A. Raghunandan, A. M. Thompson, and V. Thouret (2003), Classification of tropospheric ozone profiles over Johannesburg based on mozaic aircraft data, *Atmos. Chem. Phys.*, *3*(3), 713–723, doi:10.5194/acp-3-713-2003.
- Diab, R. D., A. M. Thompson, K. Mari, L. Ramsay, and G. J. R. Coetzee (2004), Tropospheric ozone climatology over Irene, South Africa, from 1990 to 1994 and 1998 to 2002, *J. Geophys. Res.*, *109*, D20301, doi:10.1029/2004JD004793.
- Edwards, D. P., et al. (2003), Tropospheric ozone over the tropical Atlantic: A satellite perspective, *J. Geophys. Res.*, *108*(D8), 4237, doi:10.1029/2002JD002927.
- Fishman, J., K. Fakhruzzaman, B. Cros, and D. Nganga (1991), Identification of widespread pollution in the Southern Hemisphere deduced from satellite analyses, *Science*, *252*, 1693–1696.
- Folkens, I., C. Braun, A. M. Thompson, and J. Witte (2002), Tropical ozone as an indicator of deep convection, *J. Geophys. Res.*, *107*(D13), 4184, doi:10.1029/2001JD001178.
- Garstang, M., P. D. Tyson, R. Sawp, M. Edwards, P. Källberg, and J. A. Lindesay (1996), Horizontal and vertical transport of air over Southern Africa, *J. Geophys. Res.*, *101*(D19), 23,721–23,736.
- Grodsky, S. A., and J. A. Carton (2003), The intertropical convergence zone in the South Atlantic and the equatorial cold tongue, *J. Clim.*, *16*, 723–733.
- Jacob, D. J., et al. (1996), Origin of ozone and NO_x in the tropical troposphere: A photochemical analysis of aircraft observations over the South Atlantic Basin, *J. Geophys. Res.*, *101*(D19), 24,235–24,250.
- Johnson, J. E., R. H. Gammon, J. Larsen, T. S. Bates, S. J. Oltmans, and J. C. Farmer (1990), Ozone in the marine boundary layer over the Pacific and Indian Oceans: Latitudinal gradients and diurnal cycles, *J. Geophys. Res.*, *95*(D8), 11,847–11,856.
- Kahn, R. A., W.-H. Li, C. Moroney, D. J. Diner, J. V. Martonchik, and E. Fishbein (2007), Aerosol source plume physical characteristics from space-based multiangle imaging, *J. Geophys. Res.*, *112*, D11205, doi:10.1029/2006JD007647.
- Kiviluoto, K. (1996), Topology preservation in self-organizing maps, paper presented at 1996 International Conference on Neural Networks, IEEE, Washington, D. C., doi:10.1109/ICNN.1996.548907.
- Kley, D., P. J. Crutzen, H. G. J. Smit, H. Vömel, S. J. Oltmans, H. Grassl, and V. Ramanathan (1996), Observations of near-zero ozone concentrations over the convective Pacific: Effects on air chemistry, *Science*, *274*(5285), 230–233.
- Kley, D., H. G. J. Smit, S. Nawrath, Z. Luo, P. Nedelec, and R. H. Johnson (2007), Tropical Atlantic convection as revealed by ozone and relative humidity measurements, *J. Geophys. Res.*, *112*, D23109, doi:10.1029/2007JD008599.
- Kohonen, T. (1995), The Basic SOM, in *Self-Organizing Maps*, pp. 77–130, Springer, New York.
- Krishnamurti, T. N., H. E. Fuelberg, M. C. Sinha, D. Oosterhof, N. K. Bentsman, and V. B. Kumar (1993), The meteorological environment of the tropospheric ozone maximum over the tropical South Atlantic Ocean, *J. Geophys. Res.*, *98*(D6), 10,621–10,641.
- Krishnamurti, T. N., M. C. Sinha, M. Kanamitsu, D. Oosterhof, H. Fuelberg, R. Chatfield, D. J. Jacob, and J. Logan (1996), Passive tracer transport relevant to the TRACE A experiment, *J. Geophys. Res.*, *101*(D19), 23,889–23,907.
- Lee, S., D. M. Shelov, A. M. Thompson, and S. K. Miller (2010), QBO and ENSO variability in temperature and ozone from SHADOZ (1998–2005), *J. Geophys. Res.*, *115*, D18105, doi:10.1029/2009JD013320.
- Liebmann, B., and C. A. Smith (1996), Description of a complete (interpolated) outgoing longwave radiation dataset, *Bull. Am. Meteorol. Soc.*, *77*(6), 1275–1277.
- Martin, R. V., D. J. Jacob, J. A. Logan, I. Bey, R. M. Yantosca, A. C. Staudt, Q. Li, A. M. Fiore, B. N. Duncan, and H. Liu (2002), Interpretation of TOMS observations of tropical tropospheric ozone with a global model and in situ observations, *J. Geophys. Res.*, *107*(D18), 4351, doi:10.1029/2001JD001480.
- McPeters, R. D., G. J. Labow, and J. A. Loga (2007), Ozone climatological profiles for satellite retrieval algorithms, *J. Geophys. Res.*, *112*, D05308, doi:10.1029/2005JD006823.
- Moxim, W. J., and H. Levy II (2000), A model analysis of the tropical South Atlantic Ocean tropospheric ozone maximum: The interaction of transport and chemistry, *J. Geophys. Res.*, *105*(D13), 17,393–17,415.
- Olson, J. R., J. Fishman, V. W. J. H. Kirchhoff, D. Nganga, and B. Cros (1996), Analysis of the distribution of ozone over the southern Atlantic region, *J. Geophys. Res.*, *101*(D19), 24,083–24,093.
- Oltmans, S. J., et al. (2001), Ozone in the Pacific tropical troposphere from ozonesonde observations, *J. Geophys. Res.*, *106*(D23), 32,503–32,525.
- Pfister, L., H. B. Selkirk, D. O. Starr, K. Rosenlof, and P. A. Newman (2010), A meteorological overview of the TC4 mission, *J. Geophys. Res.*, *115*, D00J12, doi:10.1029/2009JD013316.
- Phahlane, N. A. (2007), Vertical tropospheric ozone structure and associated atmospheric transport over the South African Highveld region, Master's thesis, Univ. of the Witwatersrand, S. Africa.
- Pickering, K. E., A. M. Thompson, J. R. Scala, W.-K. Tao, R. R. Dickerson, and J. Simpson (1992), Free tropospheric ozone production following entrainment of urban plumes into deep convection, *J. Geophys. Res.*, *97*(D16), 17,985–18,000.
- Pickering, K. E., et al. (1996), Convective transport of biomass burning emissions over Brazil during TRACE A, *J. Geophys. Res.*, *101*(D19), 23,993–24,012.
- Piotrowicz, S. R., H. F. Bezdek, G. R. Harvey, and M. Springer-Young (1991), On the ozone minimum over the equatorial Pacific Ocean, *J. Geophys. Res.*, *96*(D10), 18,679–18,687.
- Preston-Whyte, R. A., and P. D. Tyson (1973), Note on pressure oscillations over South Africa, *Mon. Weather Rev.*, *101*, 650–653.
- Randel, W. J., and A. M. Thompson (2011), Interannual variability and trends in tropical ozone derived from SHADOZ ozonesondes and SAGE II satellite data, *J. Geophys. Res.*, *116*, D07303, doi:10.1029/2010JD015195.
- Randriambelo, T., J.-L. Baray, and S. Baldy (2000), Effect of biomass burning, convective venting, and transport on tropospheric ozone over the Indian Ocean: Reunion Island field observations, *J. Geophys. Res.*, *105*(D9), 11,813–11,832.
- Selkirk, H. B., H. Vömel, J. M. V. Canossa, L. Pfister, J. A. Diaz, W. Fernández, J. Amador, W. Stolz, and G. Peng (2010), The detailed structure of the tropical upper troposphere and lower stratosphere as revealed by balloonsonde observations of water vapor, ozone, temperature and winds during the NASA TCSP and TC4 campaigns, *J. Geophys. Res.*, *115*, D00J19, doi:10.1029/2009JD013209.
- Smit, H. G. J., et al. (2007), Assessment of the performance of ECC-ozonesondes under quasi-flight conditions in the environmental simulation chamber: Insights from the Juelich Ozone Sonde Intercomparison Experiment (JOSIE), *J. Geophys. Res.*, *112*, D19306, doi:10.1029/2006JD007308.
- Smyth, S. B., et al. (1996), Factors influencing the upper free tropospheric distribution of reactive nitrogen over the South Atlantic during the TRACE A experiment, *J. Geophys. Res.*, *101*(D19), 24,165–24,186.
- Swap, R., M. Garstang, S. A. Macks, P. D. Tyson, W. Maenhaut, P. Artaxo, P. Källberg, and R. Talbot (1996), The long-range transport of southern African aerosols to the tropical South Atlantic, *J. Geophys. Res.*, *101*(D19), 23,777–23,791.
- Talbot, R. W., et al. (1996), Chemical characteristics of continental outflow over the tropical South Atlantic Ocean from Brazil and Africa, *J. Geophys. Res.*, *101*(D19), 24,187–24,202.
- Thompson, A. M., and R. D. Hudson (1999), Tropical tropospheric ozone (TTO) maps from Nimbus 7 and Earth Probe TOMS by the modified-residual method: Evaluation with sondes, ENSO signals, and trends from Atlantic regional time series, *J. Geophys. Res.*, *104*(D21), 26,961–26,975.

- Thompson, A. M., et al. (1993), Ozone observations and a model of marine boundary layer photochemistry during SAGA 3, *J. Geophys. Res.*, *98*(D9), 16,955–16,968.
- Thompson, A. M., K. E. Pickering, D. P. McNamara, M. R. Schoeberl, R. D. Hudson, J. H. Kim, E. V. Browell, V. W. J. H. Kirchhoff, and D. Nganga (1996), Where did tropospheric ozone over southern Africa and the tropical Atlantic come from in October 1992? Insights from TOMS, GTE TRACE A, and SAFARI 1992, *J. Geophys. Res.*, *101*(D19), 24,251–24,278.
- Thompson, A. M., W.-K. Tao, K. E. Pickering, J. R. Scala, and J. Simpson (1997), Tropical deep convection and ozone formation, *Bull. Am. Meteorol. Soc.*, *78*(6), 1043–1054.
- Thompson, A. M., B. G. Doddridge, J. C. Witte, R. D. Hudson, W. T. Luke, J. E. Johnson, B. J. Johnson, S. J. Oltmans, and R. Weller (2000), A tropical Atlantic Paradox: Shipboard and satellite views of a tropospheric ozone maximum and wave-one in January-February 1999, *Geophys. Res. Lett.*, *27*(20), 3317–3320, doi:10.1029/1999GL011273.
- Thompson, A. M., J. C. Witte, R. D. Hudson, H. Guo, J. R. Herman, and M. Fujiwara (2001), Tropical tropospheric ozone and biomass burning, *Science*, *291*(5511), 2128–2132.
- Thompson, A. M., J. C. Witte, M. T. Freiman, N. A. Phahlane, and G. J. R. Coetzee (2002), Lusaka, Zambia, during SAFARI-2000: Convergence of local and imported ozone pollution, *Geophys. Res. Lett.*, *29*(20), 1976, doi:10.1029/2002GL015399.
- Thompson, A. M., et al. (2003a), Southern Hemisphere Additional Ozone-sondes (SHADOZ) 1998–2000 tropical ozone climatology: 1. Comparison with total ozone mapping spectrometer (TOMS), *J. Geophys. Res.*, *108*(D2), 8238, doi:10.1029/2001JD000967.
- Thompson, A. M., et al. (2003b), Southern Hemisphere Additional Ozone-sondes (SHADOZ) 1998–2000 tropical ozone climatology: 2. Tropospheric variability and the zonal wave-one, *J. Geophys. Res.*, *108*(D2), 8241, doi:10.1029/2002JD002241.
- Thompson, A. M., J. C. Witte, H. G. J. Smit, S. J. Oltmans, B. J. Johnson, V. W. J. H. Kirchhoff, and F. J. Schmidlin (2007), Southern Hemisphere Additional Ozone-sondes (SHADOZ) 1998–2004 tropical ozone climatology: 3. Instrumentation, station-to-station variability, and evaluation with simulated flight profiles, *J. Geophys. Res.*, *112*, D03304, doi:10.1029/2005JD007042.
- Thompson, A. M., et al. (2010), Convective and wave signatures in ozone profiles over the equatorial Americas: Views from TC4 (2007) and SHADOZ, *J. Geophys. Res.*, *115*, D00J23, doi:10.1029/2009JD012909.
- Thompson, A. M., A. L. Allen, S. Lee, S. K. Miller, and J. C. Witte (2011a), Gravity and Rossby wave signatures in the tropical troposphere and lower stratosphere based on Southern Hemisphere Additional Ozone-sondes (SHADOZ), 1998–2007, *J. Geophys. Res.*, *116*, D05302, doi:10.1029/2009JD013429.
- Thompson, A. M., S. J. Oltmans, D. W. Tarasick, P. von der Gathen, H. G. Smit, and J. C. Witte (2011b), Strategic ozone sounding networks: Review of design and accomplishments, *Atmos. Environ.*, *45*(13), 2145–2163, doi:10.1016/j.atmosenv.2010.05.002.
- Val Martin, M., J. A. Logan, R. A. Kahn, F.-Y. Leung, D. L. Nelson, and D. J. Diner (2010), Smoke injection heights from fires in North America: Analysis of 5 years of satellite observations, *Atmos. Chem. Phys.*, *10*, 1491–1510, doi:10.5194/acp-10-1491-2010.
- Watson, C. E., J. Fishman, and H. G. Reichle Jr. (1990), The significance of biomass burning as a source of carbon monoxide and ozone in the Southern Hemisphere tropics: A satellite analysis, *J. Geophys. Res.*, *95*(D10), 16,443–16,450.
- Witte, J. C., M. R. Schoeberl, A. R. Douglass, and A. M. Thompson (2008), The quasi-biennial oscillation and annual variations in tropical ozone from SHADOZ and HALOE, *Atmos. Chem. Phys. Discuss.*, *8*, 6355–6378.
-
- A. A. Jensen and A. M. Thompson, Department of Meteorology, Pennsylvania State University, 413 Walker Bldg., University Park, PA 16802, USA. (amt16@psu.edu)
- F. J. Schmidlin, Wallops Flight Facility, NASA Goddard Space Flight Center, Wallops Island, VA 23337, USA.